

Available online at www.sciencedirect.com**ScienceDirect**

Procedia Engineering 90 (2014) 11 – 24

**Procedia
Engineering**www.elsevier.com/locate/procedia10th International Conference on Mechanical Engineering, ICME 2013

Towards Ultra-Compact High Heat Flux Microchannel Heat Sink

Jamil A. Khan*, AKMM Monjur Morshed and Ruixian Fang

*Department of Mechanical Engineering
University of South Carolina, Columbia, SC-29208, USA*

Abstract

Trends towards miniaturizing the electronics devices and to increase the computational capability has driven the modern microelectronics industry to a state where efficient thermal management issue has become the most challenging and in some case limiting parameter for the further development of these devices. Research is going on around the globe to address this challenge and to come up with a solution that is economically viable and user level applicable to meet not only the current issue but also to address the forthcoming heat removal challenges where 1000 W/cm² seems to be a feasible target specially for the defense related electronics. Exploiting high surface area to volume ratio and high latent heat of vaporization, flow boiling in microchannel possesses the highest opportunity to meet this challenge; although boiling instability and pressure fluctuation limit its implementation in any practical devices. To harness the full potential of flow boiling in microchannel, new schemes need to be implemented to control the boiling characteristics. This paper presents one active (implementation of synthetic jet in microchannel) and one passive (surface morphology modification with nanostructures) flow boiling control mechanism which can be implemented easily and can tune all the boiling performance parameters positively. Flow boiling in microchannel with reliable control mechanism could be the solution for the next generation thermal management challenges arising from the microelectronics industry.

© 2014 Published by Elsevier Ltd. This is an open access article under the CC BY-NC-ND license (<http://creativecommons.org/licenses/by-nc-nd/3.0/>).

Selection and peer-review under responsibility of the Department of Mechanical Engineering, Bangladesh University of Engineering and Technology (BUET)

Keywords: Microchannel; flow boiling; electronics cooling; synthetic jet; nanostructures.

* Corresponding author. Tel.: +0-000-000-0000 ; fax: +0-000-000-0000 .
E-mail address: khan@cec.sc.edu

1. Introduction

The challenge of heat removal is very prevalent in nature and usually crucial in many engineering applications. With the advance of the modern micro-electronics industry, efficient removal of ever increasing heat flux has become a major challenge for the thermal engineers. Heat flux of several electronics devices have already reached 100 W/cm^2 [1], which once was thought to be too high. The trends to miniaturize the electronic devices and to increase packaging density are increasing very fast specially for the defense equipment related electronics, i.e. radar, laser weapons, etc. where 1000 W/cm^2 becomes a reasonable heat removal target [2], which exceeds capability of the most advanced cooling solutions. To keep pace with the current growth trend of the microelectronics devices, efficient, reliable and user level applicable thermal management solution is necessary which is capable of dissipating large amount of heat load from a nanometer size chip with surface temperature less than a prescribed value; i.e. 125°C for defense application [3] and less than 100°C for general microelectronics.

Microchannel heat sink introduced in early 1980s by Tuckerman and Pease [4] can enhance single-phase heat transfer rate significantly compared to the conventional channel by increasing surface area to volume ratio and reducing convective heat transfer thermal resistance. However dissipation of increased heating load in single-phase convective flow in microchannel is limited by its cost, high pressure drop and high temperature gradient along the flow direction and sometimes become impractical to implement. Flow boiling in microchannel has shown great potential for the removal of high heat flux in the thermal management of the high power density electronics; it is also capable of handling dynamic and transient thermal load. However, flow boiling in microchannel is different from that of the conventional size channel [5]. Constrained by the channel walls, bubble growth for the microchannel is limited in the longitudinal direction, hence it grows rapidly both upstream and downstream. As a result, rapid bubble growth causes flow reversals, oscillations of fluid flow and system pressure. These instabilities are undesirable as they may cause problems of system control and in extreme circumstances may cause premature critical heat flux to burn out the devices. All types of instabilities; i.e. excursion instability, density wave instability, pressure drop instability and parallel channel instability, etc. [6] are undesirable and need to be eliminated.

To eliminate the unwanted flow boiling instability several attempts have been made so far mainly by introducing upstream throttling; i.e. Qu and Mudawar [7] used inlet throttling valve to eliminate the severe pressure drop oscillation, Kandlikar et al. [8] placed inlet restrictor and artificial nucleation sites, similarly, Kosar et al. [9] introduced micro fabricated inlet orifices; however throttling results in very large pressure drop. Other methods that can affect generation, expansion and condensation of bubbles in microchannel may also have the effects on stabilizing flow instabilities. This paper presents two new schemes which can be employed easily inside the microchannel to suppress or delay the boiling instability, at the same time can enhance other boiling performance parameters, i.e. reduction of surface superheat temperature for the onset of nucleation, and enhanced two-phase heat transfer coefficient (HTC). These schemes include surface morphology modifications with nanostructures which is a passive method and introduce synthetic jet inside the microchannel which acts as an active method to control flow boiling characteristics.

Surface morphology influences boiling performance very significantly. With the advent of modern ultra-fine manufacturing technology, it is now possible to control the surface morphology with nanometer scale precision. Surface morphology modifications with nanostructures may increase favorable nucleation sites density and at the same time surface wicking behavior also improved. Favorable nucleation site decrease boiling incipience temperature and wicking characteristics facilitate delivery of cool liquid to the dry out region instantly and thus delays critical heat flux. Previously surface morphology was modified with nanostructures, i.e. Si or Cu nanowires [10] or Cu nanorods [11] or carbon nanotubes [12] to enhance the pool boiling performance and encouraging results are observed. Like pool boiling, flow boiling can be controlled with the nanostructures. Efforts have been observed to use Carbon nanotubes [13], copper nanowires [14] and silicon nanopillars [15] to enhance single-phase convective flow inside microchannel. To enhance two-phase convective flow Carbon nanotubes [16] and CuNWs [17] also used previously; however the results are not totally conclusive. Besides nanostructured surfaces can serve multi-purpose objectives, i.e. Nanocomposite coating can enhance surface mechanical properties along with the boiling performance enhancement.

Synthetic jet is an active method to control the flow boiling characteristics. Unlike other active heat transfer enhancement technique, i.e. vibrating surface, stirring fluid etc. [18], synthetic jet can be easily extended to the microchannel applications. Synthetic jet has been studied extensively for the active flow control applications like jet vortices [19], control of lift and drag of airfoils [20], etc. The basic idea is to utilize the flow control aspect of the synthetic jet and use of the pulsating motion to break the elongating bubble by facilitating condensation. The formation and characterization of synthetic jets are well documented [19]. A unique feature of synthetic jets is that they are zero-net-mass-flux in nature and thus eliminating the need for additional piping and complex fluidic packaging. The other feature is that the jets strength and frequency can be adjusted by controlling the jet actuator driving signals. For thermal management application, several studies [17–19] investigated the effects of synthetic jets interacting with preexisting single-phase flow. It shows that the synthetic jet can be used to enhance the microchannel heat transfer performance by introducing turbulence into the channel flow, and modifying the flow field [21]. This strategy has rarely been studied in two-phase flow.

This paper highlights the synthetic jet and surface morphology modification (active and passive control method) effect on two-phase convective flow inside microchannel. A successful scheme to stabilize or delay the flow boiling instability with enhanced heat transfer performance will enhance its usability and make possible ultra compact heat sink design for ultra high heat flux electronic devices.

2. Experimental Facilities

The experimental setup used to conduct the experiments consists of a water supply loop, a microchannel test section and a data acquisition system. A signal generation system for driving the jet actuator was also used for the synthetic jet integration experiment.

2.1 Water Flow Loop

The test loop was an open loop configuration as presented in Fig. 1. From an inlet reservoir DI water was pumped to the test section by a gear pump (ISMATEC® Regol-z digital) which was equipped with a digital flow meter which was calibrated by the bucket and stopwatch method. A minimodule® de-gasifier was used in the flow loop to remove dissolved gases from the fluid before it enters the test section. To ensure constant inlet fluid temperature a heat exchanger, connected with a constant temperature thermal bath, was placed just before the test section.

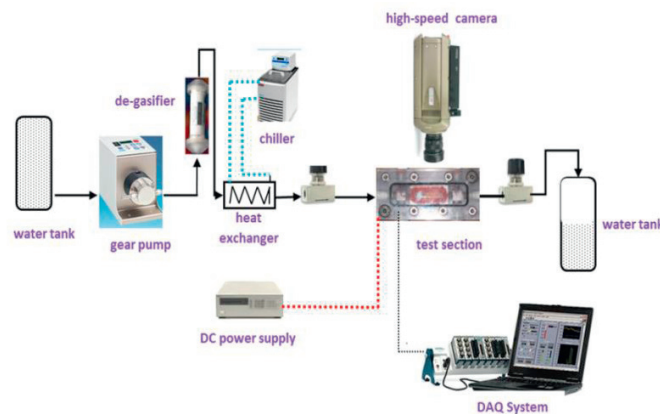


Fig. 1 Schematic diagram of the experimental setup

2.2 Test Section

The Test sections used for the experimental investigations are presented in Fig.2. The Test sections were consisted of cover plates, housing, a microchannel heat sink, a cartridge heater and insulation blocks. The microchannel heat sink is fabricated on a single copper block made from oxygen-free Cu block, the cover plate, housing block and the bottom plate were made of high temperature polycarbonate plastic, and the insulating block was made out of ceramic material.

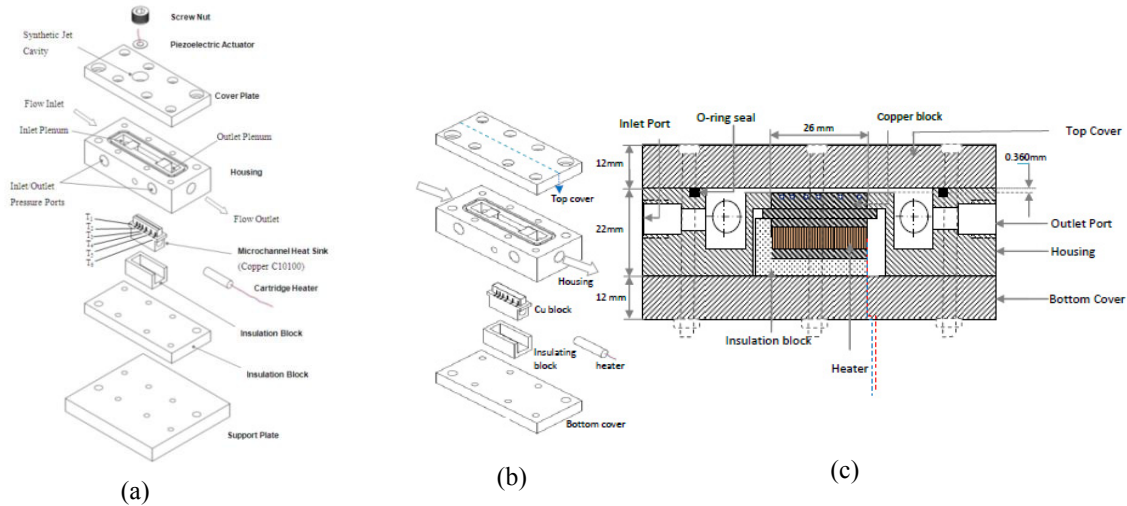


Fig.2 Schematics of the test section. (a) exploded view of the test section used for synthetic jet experiment. (b) exploded view of the test section used for surface morphology modification test. (c) Sectional view of the test section.

For the synthetic jet experiment, five parallel rectangular channels are machined into the top surface. Each channel has a dimension of $500\ \mu\text{m}$ (width) \times $500\ \mu\text{m}$ (depth) \times 26 mm (length) and the synthetic jet is formed by an array of jet orifices drilled through the bottom of the top cover plate (Fig. 2). All of orifices have the same diameter of $100\ \mu\text{m}$ and arranged into a pattern of five rows and eight columns. Due to available sample preparation facilities, size of the microchannel was different for the surface morphology modification experiment. A flat microchannel was formed by inserting the top surface of the Cu block into the cavity of the housing block (a $360\ \mu\text{m}$ (depth) \times 5 mm (width) \times 26 mm micro-channel is formed). 3 mm below the top surface, holes with diameter of 0.85 mm are drilled into the side wall up to the half width of the copper block to accommodate type-K thermocouples. A 100W cartridge heater was inserted into the hole of the Cu block to provide heat to the microchannel. Thermal resistance between heater surface and the Cu block was minimized applying a thermal compound (Artic Silver[®] 5) on top of the heater surface. The heater was powered by a DC power supply.

2.3 Data Acquisition

Thermocouples were inserted into the holes of the Cu block. Surface temperatures of Cu were determined from the temperature readings of these thermocouples. Inlet and outlet temperatures were also measured to calculate the heat carried by the flowing fluid. Two pressure transducers (Omegadyne PX 309) were also connected with the inlet and outlet plenum to measure the absolute pressure. A NI compact DAQ-9172 data acquisition system and LabVIEW program were used to record all pressure and temperature data.

2.4 Flow Visualization System

A high speed CCD camera (Phantom v7.3) with microlens is used for the flow boiling visualization. At 800×600 resolutions, the camera has a maximum frequency of 6688 frames-per-second.

3. Experimental Procedure and Data Processing

3.1 Experimental Procedure

To perform the experiment, the test section was assembled and connected in the flow loop. Inlet temperature was adjusted and the pump was set to run at a desired flow rate. Once the flow rate and inlet temperature were stabilized, a predetermined level of power was supplied to the heater. Temperature and pressure of the test section were monitored until it reached steady state. Once the system is in steady state, temperature, pressure and input power data were recorded and the power was increased at a step of ~5V. The experiment was carried out for a fixed flow rate and with different input power until the system reaches critical heat flux condition.

3.2 Data Reduction

For the single-phase and sub-cooled two-phase heat transfer, the steady-state sensible heat gain Q by the coolant can be determined from an energy balance:

$$Q = \rho C_p (T_{in} - T_{out}) \dot{Q} \quad (1)$$

Where, \dot{Q} is the volumetric flow rate (measured from the pump control panel), density (ρ) and specific heat (C_p) have been obtained using fluid mean temperature (T_m).

$$T_m = (T_{in} + T_{out})/2$$

In this experiment, voltage (V) and current (I) were measured directly from the power supply and input power (Q_{in}) to the cartridge heater was calculated.

$$Q_{in} = V.I \quad (2)$$

Depending on the flow rate, 80 ~90 % of the input power was carried by the flowing water. Heat losses from the experimental setup have been calculated by subtracting the energy gained by the water from the total electrical power input.

$$Q_{loss} = P_{in} - Q_p C_p (T_{in} - T_{out}) \quad (3)$$

Effective heat flux was calculated using

$$q_{eff} = (P_{in} - Q_{loss})/A_t \quad (4)$$

Where, A_t is heat transfer area (26 mm × 5 mm for the flat microchannel and 26 mm × 5.5 mm for the parallel microchannel). For boiling with saturation exit, q_{eff} was calculated using Q_{loss} of the single-phase liquid exit.

Surface temperature of the heat sink were estimated from 1D steady state conduction equation coupled with the thermocouple's reading (thermocouples were inserted into the copper block).

$$T_{i,s} = T_i - Q \cdot t / K_{cu} \cdot A_t \quad (5)$$

Where, $T_{i,s}$ is the surface temperature at different locations, T_i is the corresponding thermocouple reading, K_{cu} is the thermal conductivity of the copper block (391 W/m.K), t is the distance between thermocouple position and top surface (3 mm).

Average surface temperature and effective heat flux has been calculated using

$$T_s = (T_{1,s} + T_{2,s} \dots + T_{n,s}) / n \quad (6)$$

Average single-phase heat transfer coefficient was calculated using:

$$h_{sp} = q_{eff} / (T_s - T_m) \quad (7)$$

Once fluid reaches saturated condition at the exit, microchannel can be divided into two regions: upstream subcooled region and downstream saturated region and location of the zero thermodynamic equilibrium quality marks the dividing point [22]. Length of these two regions was evaluated using:

$$L_{sub}^* = L_{sub} / L = m C_p (T_{sat} - T_{in}) / (P_{in} - Q_{loss}) \quad (8)$$

$$L_{sat}^* = 1 - L_{sub}^*$$

Fluid temperature of the channel was calculated using:

$$T_f = (T_{in} + T_{out}) / 2 \quad (\text{if } L_{sub}^* \geq 1) \\ T_f = (T_{in} + T_{sat}) / 2 \times L_{sub}^* + T_{sat} \times L_{sat}^* \quad (\text{if } L_{sub}^* < 1) \quad (9)$$

Average two-phase heat transfer coefficient was calculated using:

$$h_{tp} = q_{eff} / (T_s - T_f) \quad (10)$$

3.3 Uncertainty Analysis

Uncertainties associated with the instruments were: flow rate $\pm 0.02\%$, current $\pm 0.06\%$, voltage $\pm 0.15\%$, local temperature $\pm 0.5^\circ\text{C}$ and differential pressure $\pm 0.25\%$. Uncertainty propagation in the calculated value was computed by Kline and McClintock method [23]. Uncertainties in the mass velocity and effective heat flux are calculated as $\pm 3.4\%$, $\pm 5\sim 17\%$ depending on the flow conditions.

4. Results and Discussion

4.1 Effect of Synthetic Jet

To examine the effect of the synthetic jet, a unimorph type piezoelectric actuator is employed as the active part of the synthetic jet actuator and placed over the orifice arrays. The resonance frequency of the actuator itself is 2.6 kHz. To operate the synthetic jet a signal generation system is designed to supply sinusoidal signal to drive the piezoelectric actuator. It includes a direct digital synthesis function generator (BK Precision model 4007DDS) and a wide band power amplifier (Krohn-Hite model 7602M).

Microchannel used in heat transfer application generally operates in the laminar region. As we already know, heat transfer in laminar flow is much lower compared to the turbulent flow due to lower mixing of cold and hot fluid and thicker boundary layer. Heat transfer rate also varies significantly between developed flow and developing flow

region. In the developing flow region thermal boundary layer is much thinner. As a result, steep temperature gradients are created and heat transfer rate is improved. Operation of synthetic jet sucks working fluid into the jet cavity through the orifices and then rapidly expelled out and thus modifies the channel flow fields near the jet orifices. Those micro jets penetrate the main microchannel stream and impinge on the heated channel wall, thus the thermal boundary layer near the wall gets much thinner. As a result, steep temperature gradients are created at the heated channel wall and heat transfer rate is improved accordingly. Fig. 3 establishes that fact; heat transfer rates get enhanced with the synthetic jet. It is also to mention that the channel flow rates play an important role on the thermal performance of the synthetic jets. For instance, when the channel flow Reynolds number is at 96, the heat transfer coefficient is enhanced by ~138% compared to the channel without synthetic jet. While for the channel flow Reynolds number at 467, the heat transfer augmentation is ~55%. As illustrated in Fig. 3, there is a rapid decrease of the enhancement with increasing Reynolds number and it is mainly attributed to that the jet-to-channel stream momentum ratio decreases rapidly as channel flow rate increasing.

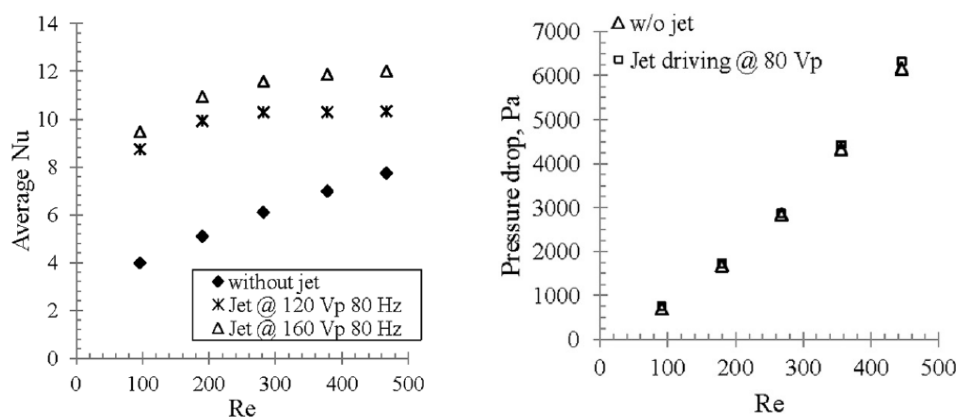


Fig. 3 : Effect of synthetic jet on microchannel heat transfer in single-phase flow

It is expected that changing the jet strength by changing the input voltage will change their ability to affect the heat transfer performance in microchannels. Generally, stronger jets will introduce intense disturbance into the channel flow stream, thus the degree of heat transfer enhancements can be adjusted by controlling the synthetic jets strength as also illustrated in Fig. 3. A mathematical model was developed and numerically solved using FLUENT to understand different parameters inside the microchannel due to flow modifications. Though the above analysis, it can be seen that the synthetic jet periodically interrupts the micro-channel flow and breaks up the developing thermal and hydrodynamic boundary layers at the heated channel wall. This cross-flow interaction creates steep velocity and temperature gradients at the heated surface as long as jet impingement occurs. This pulsating low mechanism therefore leads to improved thermal performances in the hybrid cooling scheme of micro-channel and synthetic jet. Jet affected length over a full cycle can be also estimated; the time-averaged local Nusselt number is plotted against the channel length and compared with the baseline value, as shown in Fig. 4. For this specific operating condition, the most effectively affected length is around 5 mm down from the jet orifice.

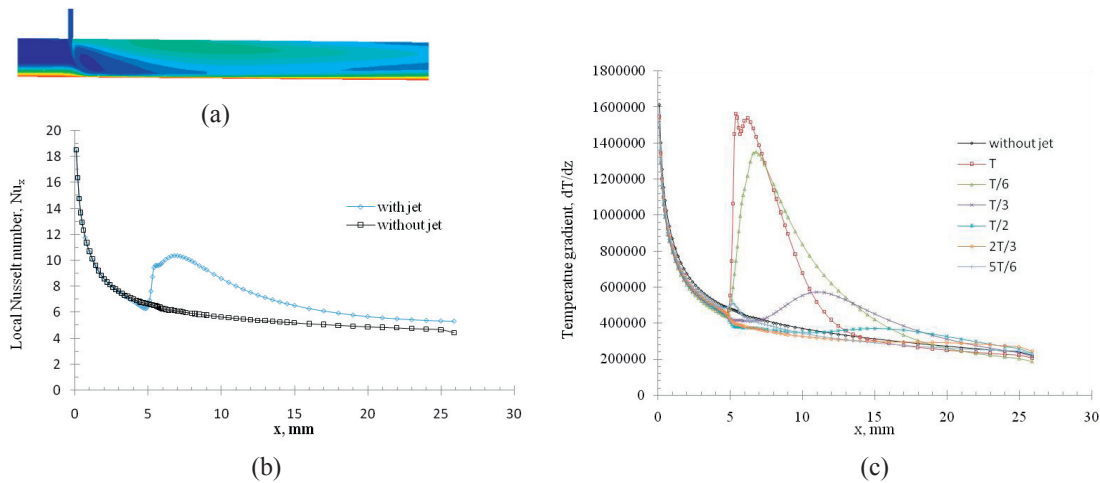
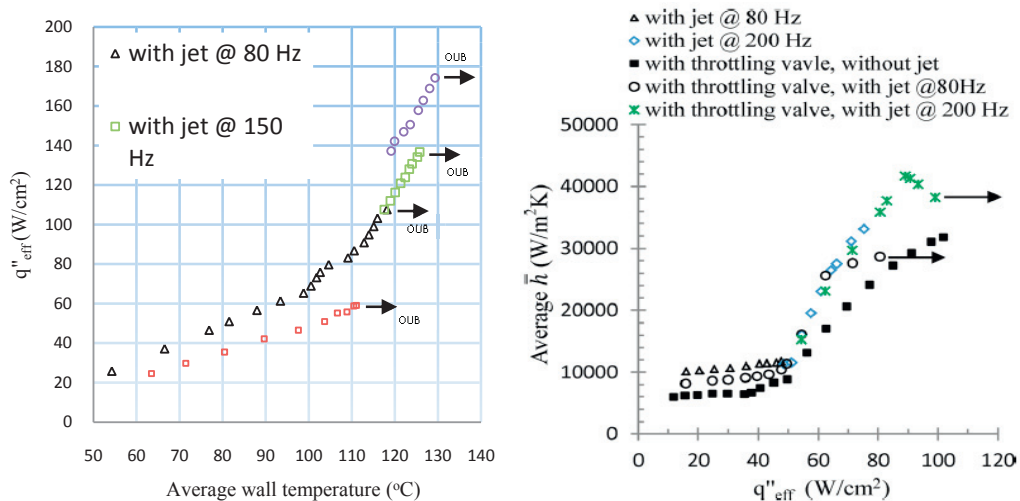


Fig. 4 : (a) temperature field variation along the channel length (b) time-averaged local Nusselt number with synthetic jet (c) Time-lapsed temperature derivatives over z at the channel bottom wall for one cycle.

In microchannel, as the heat flux increases surface temperature of the channel also increases linearly and at an elevated heat flux there is high temperature gradient in the axial direction. Depending on the fluid inlet temperature, a portion of the microchannel will have single phase flow and then the boiling is initiated from the downstream region. Operation of the synthetic jet in this early stage of boiling mainly contributes to the flow field modification in the channel which contributes to the overall heat transfer coefficient enhancement. Synthetic jet also has predominant effect on the bubble dynamics during nucleate boiling.

Due to operation of the synthetic jet, the channel pressure field is changed in a periodic manner, and net momentum is introduced into the channel flow and thus forces balancing between the surface tension, inertia force, and the net force due to the evaporation momentum are changed. The jet introduced momentum may help to push the nucleating bubble to downstream during the expelling stroke, and attract the bubble to upstream during the suction stroke. In either way, it causes the bubble detaching at a different rate and thus bubble nucleation rate also increases. As a result, heat transfer rate increases in two-phase region as can be seen in Fig. 5.



(a) (b)

Fig. 5 : (a) Boiling curve with synthetic jet operation (b) effect of the synthetic jet on two-phase heat transfer coefficient.

As the heat flux increases nucleation sites density and bubble growth rates also increases. Bubble grows and merge with each other before they are swept away by the flowing liquid. As the bubble growth constrained by the side wall only allowed growing in upstream and downstream directions only, this blocks further liquid to cool the heated region and thus triggers the critical heat flux.

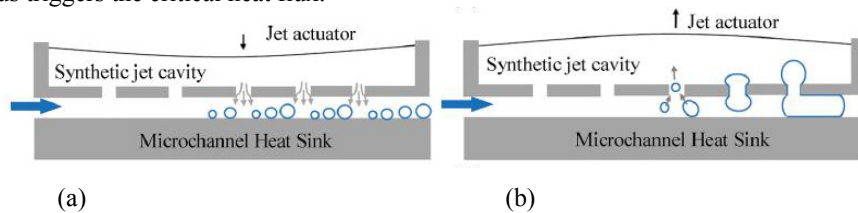


Fig. 6: Mechanism of using synthetic jets to suppress flow boiling instabilities: (a) Bubble collapse during the discharge stroke; (b) Bubble collapse during the suction stroke.

Operation of the synthetic jet can break the elongating bubbles by two distinct physical phenomena. During the ejection stroke of each cycle relatively cold fluid (due to mixing of upstream and downstream fluid inside the jet cavity) impinges on the bubble to collapse it (as can be seen in Fig. 6(a)). Again during the suction stroke as shown in Fig. 6(b), bubbles can be sucked into the jet cavity and mixes with the upstream relatively cold liquid and condensed. Synthetic jet strength and its operation frequency both affect the boiling instability. With the increase of frequency critical heat flux increases as can be seen from Fig. 5. Jet location, Jet orifice size, Jet Strength and Jet Frequency; all these parameters affect instability mitigate mechanism and thus need to be optimized depending the cooling liquid, geometric dimension of the channel and liquid velocity.

4.2 Effect of Surface Modification with Nanostructures

Surface roughness can enhance convective heat transfer in single-phase microchannel flow [24]. To explore the effect of the nanostructures, surface morphology of the microchannel was modified with copper nanowires (CuNWs) and Cu-Al₂O₃ nanocomposite. Template based electrochemical synthesis technique [25] was used to synthesis CuNWs on the top surface of the Cu block. The Cu-Al₂O₃ nanocomposite coating was developed on the top surface of the copper heat sink using electrocodeposition technique [26].

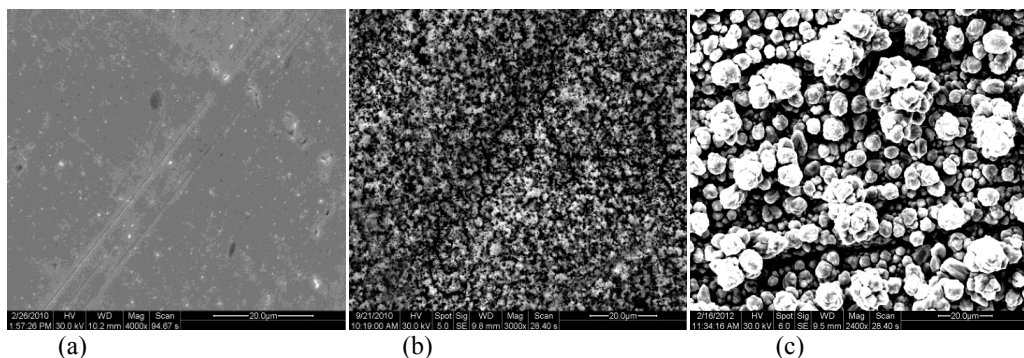


Fig. 7. Scanning electron microscopy (SEM) graphs of (a) top view of bare Cu surface (b) top view of Cu nanowires (c) top view of the Cu-Al₂O₃ nanocomposite coating

Scanning electron microscopy (FEI Quanta 200 SEM) was used to characterize surface morphology of the modified surfaces and compared with the bare Cu surface. Fig. 7 presents the top view of the bare Cu surface,

CuNWs coated surface and CuAl_2O_3 nanocomposite coated surface. Micro scale surface roughness and different micro size surface cavity developed on the copper surface due to the coating which facilitates nucleation.

Nanostructure coated surface is expected to be more effective in boiling heat transfer, albeit its effect on single-phase flow is also encouraging. CuNWs coated surface was investigated in single-phase flow. Heat transfer rate increases for the nanowires coated surface compare to the bare surface as indicated in Fig.8. However, the effect becomes less significant with the increase of Reynolds number. This enhancement plausibly attributed to the fin effect of the nanostructured surfaces; and with the increase of Reynolds number heat transfer coefficient of the channel increases. According to the conventional fin theory, fin effectiveness reduces as the heat transfer coefficient increases.

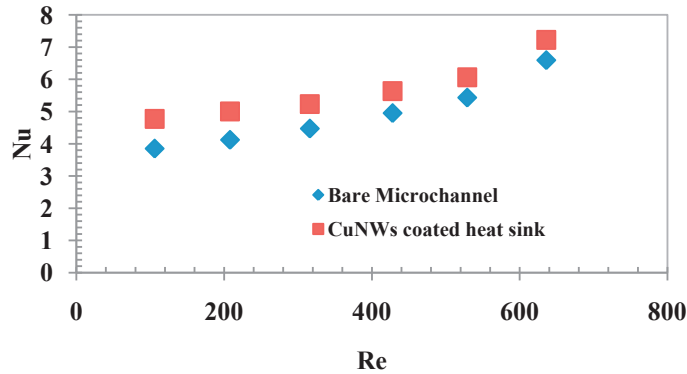
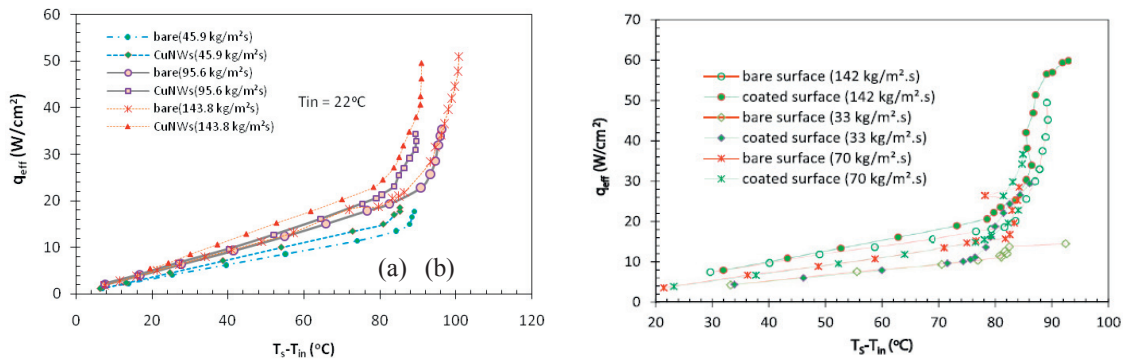


Fig. 8 : Effect of CuNWs Coating on Single-phase heat transfer in microchannel

Although nanostructures coated surface have considerable positive effect in single-phase flow but its real impact can be observed in two-phase flow. Two phase flow is mostly characterized with three parameters: surface superheat temperature required for the onset of bubble nucleation (ONB), two-phase heat transfer coefficient (HTC), and critical heat flux (CHF) or onset of unstable boiling (OUB). Nanostructures coated surface can influence all of these parameters. Fig. 9 presents the boiling curves and two-phase heat transfer coefficient for the nanostructured surfaces compared with that of the bare surface.



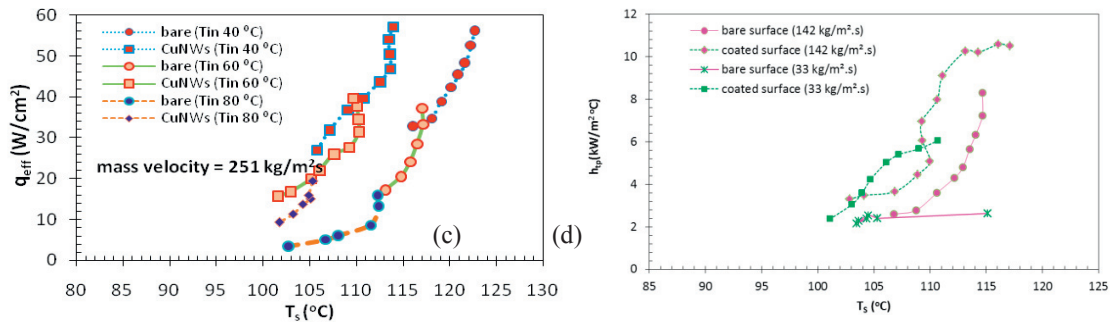


Fig. 9 : Boiling Curve for the (a) CuNWs coated surface compared to the bare surface; (b) Cu-Al₂O₃ nanocomposite coated surface compared to bare surface (c) Effect of inlet temperature on boiling Curve. (d) two-phase heat transfer coefficient for the Cu-Al₂O₃ nanocomposite coated surface compared to the bare surface

As can be seen from the Fig.9, in the single-phase zone, surface temperature rises almost linearly with the heat flux and single-phase HTC is slightly higher for the nanostructured surfaces compared to the bare surface. Once the boiling initiates, most of the heat is carried by the coolant utilizing latent heat of vaporization instead of single-phase sensible heat gain; as a result slope of the boiling curve starts to be steeper from the boiling incipient point which indicates a sharp rise in HTC. Boiling starts or bubble nucleates generally from the artificial or natural cavity presents on the boiling surface; comparatively large size cavity becomes active earlier than smaller size cavity [18]. Nanostructured coated surface has larger cavity compared to the bare surface as can be seen in Fig. 7; as a result bubble nucleates earlier for the nanostructured surface. For the experimental condition, boiling was observed to initiate 3 to 8 °C earlier for the coated surface compared to the bare surface and nanostructures coated surface was 8 to 12 °C cooler than the bare surface during the entire boiling experiment.

Two-phase HTC has been found significantly higher for the coated surface compared to the bare surface as can be seen in Fig. 9 (d). Depending on the surface temperature, flow rate and coating type, ~30% to ~120% enhancement in two-phase HTC was observed. This enhancement in two-phase HTC is attributed to the surface morphological modifications and two-phase flow pattern inside the channel. At comparatively low heat flux bubbles initiate on the solid surface, grow and are lifted off by the flowing liquid and condense immediately in the sub-cooled liquid; in this nucleate boiling regime, increased nucleation site density plausibly cause the enhancement in two-phase HTC. This nucleate boiling regime doesn't last long in micro channel due to space constrained in the lateral direction. At high heat flux bubbles grow very quickly and merge with each other before they are swept away. As these larger vapour bubbles are confined between side walls, they form an elongated vapour slug which grows in both upstream and downstream directions and is flushed out by the liquid. These cycles repeat and with the increase of the heat flux the frequency of this vapour slug increases. This pulsating elongated bubbly flow regime is found to dominate in the flow boiling of this channel. In the elongated bubble regime a thin liquid film exists at the bottom of the bubble; transient evaporation of this thin liquid film is identified as the dominant heat transfer mechanism of this regime [19]. Evaporation rate increases for the nanostructured surface compared to the bare surface [20]; additionally the structured surface facilitates better liquid transport to the evaporation site utilizing enhanced surface capillarity. All these effects cause better HTC for the nanostructured surfaces. With the increase of inlet temperature, nucleation sites become active earlier, resulting in a decrease of boiling incipient temperature, having high density favourable nucleation sites, nanostructured surfaces become more effective with the increase of inlet temperature.

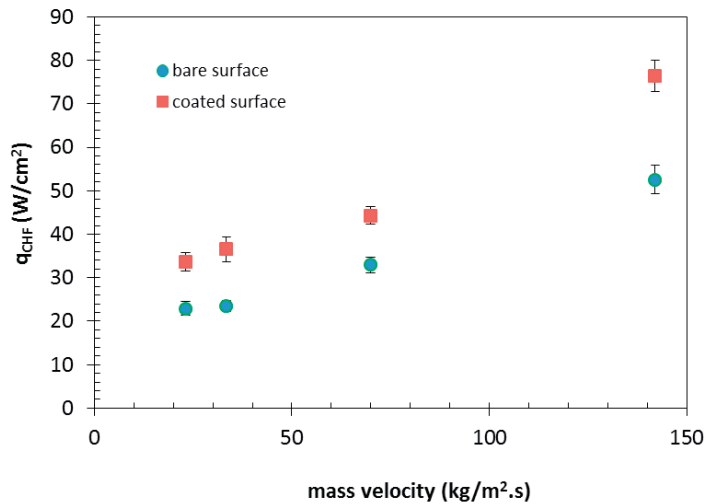


Fig. 10. Critical heat flux for different mass flow rate.

Another important consideration for the flow boiling performance is the critical heat flux (CHF). CHF indicates maximum heatflux that can be handled with the operating parameters. In many cases of the microchannel experiment, immature CHF is triggered by the vapour backflow [8]. Immature CHF has been minimized in this study by introducing a flow restrictor in the inlet port and by reducing the flexible hose size of the outlet. CHF in a microchannel takes place due to local dry out and it increases with the mass flow rate. Fig. 10 presents critical heat flux obtained for different mass flow rates for the Cu-Al₂O₃ nanocomposite coating. As can be seen from Fig. 10, CHF increases for the coated surface compared to the bare surface; in this study up to 55% enhancement in the CHF has been observed for the coated surface. Plausible reason of this enhancement is related with the surface wettability and wicking characteristics. Nanocomposite coating increases the surface wettability which expedites spreading of the liquid to the dry out region as illustrated in Fig. 11, resulting in increased CHF.

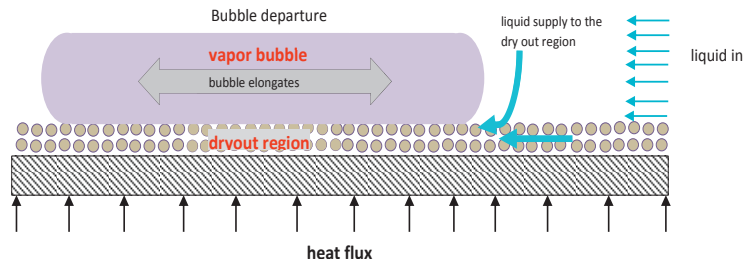


Fig. 11 : CHF enhancement mechanism for the nanostructured surfaces

4.3 Other Methods for Controlling Two-phase flow in Microchannel:

Several other techniques also have been applied so far for the enhancement of single-phase flow in microchannel which includes both passive and active techniques. Passive techniques include surface roughness, flow disruptions, pin fins, offset-strip fins, channel curvature, re-entrant, obstructions, secondary flows, out-of-plane mixing, and nanofluids; among the active techniques vibration of side walls, electrostatic fields, flow pulsation, and variable roughness structures have been also used. Some of these techniques also have been used for the two-phase flow in microchannel and mixed results have been observed; i.e. Nanofluids have been studied and modest improvements have been observed but deposition of particles and thereby channel clogging limits its application.

Active oscillatory mass flow controller to reduce the flow oscillations was proposed by Zhang et al [27]. Application of micropin fin array can enhance two-phase CHF but the cost of pressure drop limits its application, Surface modifications with re-entrant cavities can also meet the demand of boiling performance improvement.

5. Conclusions

Two-phase microchannel cooling with reliability and enhanced performance is an important and viable means to mitigate the forthcoming heat removal challenges. To ensure the reliable operation and to harness the full potential of two-phase microchannel cooling, innovative schemes are necessary which can control the system behaviour and at the same time can enhance heat transfer rate and CHF. In this paper two promising and representative active and passive techniques have been explored and their thermo-hydraulic benefits have been discussed.

Synthetic jet is a very promising dynamic control technique which can control the oscillatory behaviour where reliable operation is of critical importance. However synthetic jet is also very effective in enhancing both single-phase and two-phase heat transfer by introducing turbulence and modifications of bubble dynamics inside the microchannel. With the oscillatory motion of the synthetic jet, bubble expansion characteristics also changes to enhance CHF. Synthetic jet is very effective in microchannel heat transfer but its effect becomes more profound to address local hot spots and transient heat load.

Surface morphology modification with nanostructures is a very effective passive technique. Application of precisely designed nanocoating can alter surface properties to suit boiling performance improvement. Reduction in boiling incipient temperature, increase in boiling heat transfer coefficient and also increase in CHF also are observed for the nanocoated surface. Reliable and economically justifiable nanocoating that can be applied inside the microchannel wall will keep exploring to bring a paradigm shift in two-phase microchannel cooling.

Two-phase microchannel with reliable active and passive control techniques can be successfully employed to dissipate a large heat load from a very limited space and help sustain the exponential growth of the modern microelectronics innovation.

References

- [1] Bar-Cohen, A., P. Wang, and E. Rahim, *Thermal management of high heat flux nanoelectronic chips*. Microgravity Science and Technology, 2007. **19**(3): p. 48-52.
- [2] Mudawar, I., et al., *Two-Phase Spray Cooling of Hybrid Vehicle Electronics*. Components and Packaging Technologies, IEEE Transactions on, 2009. **32**(2): p. 501-512.
- [3] Jaeseon, L. and I. Mudawar. *Low-temperature two-phase micro-channel cooling for high-heat-flux thermal management of defense electronics*. in *Thermal and Thermomechanical Phenomena in Electronic Systems, 2008. ITherm 2008. 11th Intersociety Conference on*. 2008.
- [4] Tuckerman, D.B. and R.F.W. Pease, *High-Performance Heat Sinking for VLSI*. Electron Device Letters, 1981 **2**(5): p. 126-129.
- [5] Bhide, R.R., et al., *An active control strategy for reduction of pressure instabilities during flow boiling in a microchannel*. Journal of Micromechanics and Microengineering, 2011. **21**(3): p. 035021.
- [6] Lu, C.T. and C. Pan, *Stabilization of flow boiling in microchannel heat sinks with a diverging cross-section design*. Journal of Micromechanics and Microengineering, 2008. **18**(7): p. 075035.
- [7] Qu, W. and I. Mudawar, *Measurement and prediction of pressure drop in two-phase micro-channel heat sinks*. International Journal of Heat and Mass Transfer, 2003. **46**(15): p. 2737-2753.
- [8] Kandlikar, S.G., et al., *Stabilization of Flow Boiling in Microchannels Using Pressure Drop Elements and Fabricated Nucleation Sites*. Journal of Heat Transfer, 2005. **128**(4): p. 389-396.
- [9] Koşar, A., C.-J. Kuo, and Y. Peles, *Suppression of Boiling Flow Oscillations in Parallel Microchannels by Inlet Restrictors*. Journal of Heat Transfer, 2005. **128**(3): p. 251-260.
- [10] Chen, R., et al., *Nanowires for Enhanced Boiling Heat Transfer*. Nano Letters, 2009. **9**(2): p. 548-553.
- [11] Li, C., et al., *Nanostructured Copper Interfaces for Enhanced Boiling*. Small, 2008. **4**(8): p. 1084-1088.
- [12] Ujeh, S., T. Fisher, and I. Mudawar, *Effects of carbon nanotube arrays on nucleate pool boiling*. International Journal of Heat and Mass Transfer, 2007. **50**(19-20): p. 4023-4038.
- [13] Dietz, C., *Single phase forced convection in a microchannel with carbon nanotubes for electronic cooling applications* in *Mechanical*. 2007, Georgia Institute of Technology.
- [14] Ali, M.Y., *Experimental investigation of the effect of copper nanowires on heat transfer and pressure drop for a single phase microchannel*, in *Mechanical Engineering*. July 2010, University of South Carolina: Columbia, South Carolina, USA. p. 53.
- [15] Dixit, P., et al., *Silicon nanopillars based 3D stacked microchannel heat sinks concept for enhanced heat dissipation applications in MEMS*

- packaging. Sensors and Actuators A: Physical, 2008. **141**(2): p. 685-694.
- [16] Khanikar, V., I. Mudawar, and T. Fisher, *Effects of carbon nanotube coating on flow boiling in a micro-channel*. International Journal of Heat and Mass Transfer, 2009. **52**(15-16): p. 3805-3817.
- [17] Morshed, A.K.M.M., et al., *Enhanced flow boiling in a microchannel with integration of nanowires*. Applied Thermal Engineering, 2012. **32**(0): p. 68-75.
- [18] Steinke, M.E. and S.G. Kandlikar, *Review of single-phase heat transfer enhancement techniques for application in microchannels, minichannels and microdevices*. International Journal of Heat and Technology, 2004. **22**(2): p. 3-11.
- [19] Smith, B. and A. Glezer, *Jet vectoring using synthetic jets*. Journal of Fluid Mechanics, 2002. **458**(1): p. 1-34.
- [20] Smith, D.R., et al., *Modification of lifting body aerodynamics using synthetic jet actuators*. AIAA paper, 1998. **209**: p. 1998.
- [21] Fang, R., *EXPERIMENTAL AND NUMERICAL ANALYSIS OF ENHANCED MICRO-CHANNEL COOLING USING MICRO-SYNTHETIC JETS*, in *Mechanical Engineering*. 2011, University of South Carolina.
- [22] Qu, W. and I. Mudawar, *Flow boiling heat transfer in two-phase micro-channel heat sinks—I. Experimental investigation and assessment of correlation methods*. International Journal of Heat and Mass Transfer, 2003. **46**(15): p. 2755-2771.
- [23] Holman, J.P., *Experimental methods for engineers*. 6th ed. 1994: McGraw-Hill.
- [24] Kandlikar, S.G., et al., *Heat Transfer in Microchannels—2012 Status and Research Needs*. Journal of Heat Transfer, 2013. **135**(9): p. 091001-091001.
- [25] Gao, T. and et al., *Electrochemical synthesis of copper nanowires*. journal of physics: Condensed Matter, 2002. **14**(3): p. 355.
- [26] Allahkaram, S.R., S. Golroh, and M. Mohammadipour, *Properties of Al₂O₃ nano-particle reinforced copper matrix composite coatings prepared by pulse and direct current electroplating*. Materials & Design, 2011. **32**(8-9): p. 4478-4484.
- [27] Zhang, T. J., Peles, Y., Wen, J. T., Tong, T., Chang, J. Y., Prasher, R., Jensen, M. K., Analysis and active control of pressure-drop flow instabilities in boiling microchannel systems, International Journal of Heat and Mass Transfer, 53 (2010) 2347–2360.